Crystal Structure Explains Crystal Habit for the Antiviral Drug Rimantadine Hydrochloride

Anatoly Mishnev and Dmitrijs Stepanovs

Latvian Institute of Organic Synthesis, Aizkraukles 21, Riga, LV-1006, Latvia

Reprint requests to Dr. Anatoly Mishnev. Fax: +371 67014801. E-mail: mishnevs@osi.lv

Z. Naturforsch. **2014**, *69b*, 823 – 828 / DOI: 10.5560/ZNB.2014-4075
Received April 11, 2014

The crystal structure of the antiviral drug rimantadine hydrochloride, $C_{12}H_{22}N^+$ Cl^-, has been elucidated by a single-crystal X-ray structure analysis. The structure consists of 1-(1-adamantyl)ethanamine (rimantadinium) cations and chloride anions. The Cl^- anions link the rimantadinium cations *via* N–H···Cl hydrogen bonds into infinite rectangular chord-like structural units with charged groups in the inner channel and aliphatic groups on the surface, and oriented along the unit cell *c* axis. In contrast to strong electrostatic and hydrogen bonding inner interactions the chords in the crystal are held together by weak van der Waals forces only. A two-fold symmetry axis passes through the center of the chord. By indexing of the crystal faces it has been shown that the maximal dimension of the needle-like crystals coincides with the direction of the unit cell *c* axis. These structural features explain the crystal habit and the anisotropy of the mechanical properties of rimantadine hydrochloride crystals observed upon slicing and cleavage.

Key words: Rimantadine Hydrochloride, Antiviral Drug, X-Ray Diffractometry, Crystallinity, Crystal Shape, Aspect Ratio

Introduction

Influenza viruses are major causative agents of severe respiratory diseases leading to huge medical and economical losses in annual epidemics and periodic pandemics. Currently two classes of antivirals are approved for prophylaxis and treatment of influenza: M2 ion channel blockers and neuraminidase inhibitors [1, 2]. Rimantadine ((*RS*)-1-(1-adamantyl)ethanamine) as well as its analog amantadine (adamantan-1-amine) bind to M2 proton channels and blocks the influx of H^+ ions into the virion, a process essential for the uncoating stage of the viral replication cycle [3].

Rimantadine hydrochloride (**Rim HCl**) (Fig. 1) has been used as a medicinal product for over 40 years. Despite this fact, till present, the molecular and crystal structure of the compound has not been investigated. As can be seen from Fig. 2, crystals of **Rim HCl** have a needle-like shape with high aspect ratio. Since crystals were too long for analyzing them as they were grown, we had to cut them into shorter pieces to fit the diameter of the X-ray beam. However, we observed that the cut edges of the crystals were stratified. Cracking of the crystals resulted in their bursting into smaller needles with similar aspect ratio. In spite of a big enough size and transparency the crystals of **Rim HCl** for some reason exhibited low X-ray diffraction quality. Usually application of low temperatures gives rise to better accuracy of the diffraction experiment, but in the case of **Rim HCl** crystals, exposing them to low temperatures (150 – 180 K), resulted in an increase of sample mosaicity. These two facts let us suggest that such an unusual behavior of samples, and the problems faced in the process of the crystal structure determination, could be related to the packing of struc-

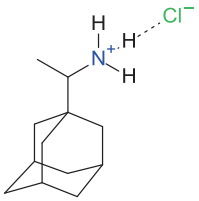

Fig. 1. Structural formula of **Rim HCl**.

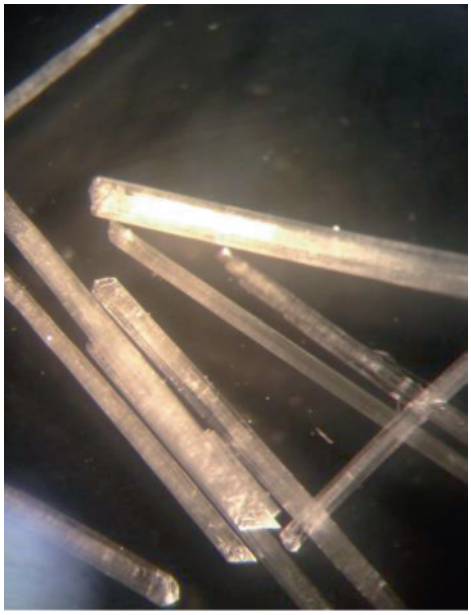

Fig. 2. Needle-shaped crystals of **Rim HCl**.

tural units. Thus the purpose of this study was not only to determine the unknown crystal structure of a well-known drug, but also to explain the shape of the crystals and their anisotropy in mechanical properties observed upon slicing and cleavage.

The shapes of crystals obtained by crystallization from solution and the mechanical properties of drugs (brittleness, compactibility, flowability) usually play an important role in the pharmaceutical industry defining material properties of dosage forms [4]. Needle-shaped crystals, *i. e.* crystals with large aspect ratio, are commonly encountered in the pharmaceutical and fine chemicals industries. To fight these harmful phenomena some methods were developed for breakage of the crystal growth process. Bao *et al*. [5] presented a model of L-threonine crystals describing their growth and binary breakage. Biscans [6] studied the breakage of monosodium glutamate crystals by using attrition. Attempts to robotize modification of the crystal shape invoked the development of methods for particle-size monitoring and the control of crystallization processes [7]. There are theoretical approaches in the literature for the prediction of crystal morphologies from crystallographic X-ray data [8]. A knowledge of the crystal surface structure on the molecular level is crucial for an understanding of the physical and chemical properties. In order to determine and characterize the surface structure of particular crystal faces, the molecular packing and the face indices must be properly assigned [9, 10].

Results and Discussion

A view of the **Rim HCl** structure and the atomic numbering are given in Fig. 3.

The C–C bonds of the adamantane system range from 1.467(9) to 1.551(8) Å with a mean value of 1.505 Å, which is lower than the average value of 1.535 Å for the C(sp^3)–C(sp^3) bond in hexane. Reduction of the C(sp^3)–C(sp^3) bond lengths in the adamantane ring system is due to positional disorder caused by rotation around the C_3 axis of the adamantyl moiety. The C–C–C bond angles, with a mean value of 109.5°, are in good agreement with the value for the tetrahedral angle. The individual values vary from 106.5(5) to 111.5(6)°. The bond lengths in the ethanamine substituent are: N2–C4 = 1.476(5) Å, C3–C4 = 1.521 (5) Å and C4–C5 = 1.532 (4) Å. These values are close to the standard values [12].

In the crystal the protonated amino group forms N–H···Cl hydrogen bonds (H bond) with three neighboring chloride anions (Table 1). The orientations of these H bonds coincide with directions of the unit cell vectors c, $a + b$ and b–a, respectively. The two latter H bonds link four rimantadinum cations *via* Cl^- anions into a rectangular subunit perpendicular to the c axis, while the first one associates these rectangular subunits into an infinite chord-like arrangement with charged groups in the inner channel and aliphatic groups on the surface, and oriented along the unit cell c axis

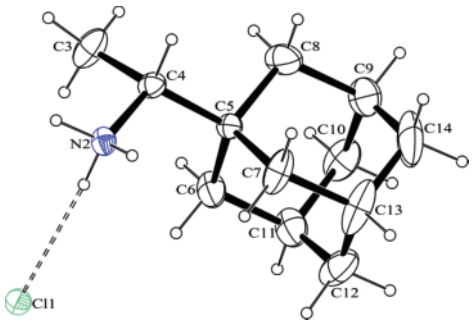

Fig. 3. ORTEP-III [11] drawing of the molecular structure of **Rim HCl** in the crystal showing the adopted atom labelling scheme. Displacement ellipsoids are drawn at 30 % probability and H atoms as spheres with arbitrary radius.

D–H···A	D–H	H···A	D···A	∠D–H···A	Symmetry operator
N2–H2*A*···Cl1	0.88	2.29	3.158(3)	168	
N2–H2*B*···Cl1	0.88	2.32	3.163(3)	152	$-0.5+y, 0.5+x, 0.5+z$
N2–H2*C*···Cl1	0.86	2.38	3.195(3)	152	$0.5+y, 0.5-x, 0.5+z$

Table 1. Hydrogen bond geometry (Å, deg).

(Figs. 4a and 4b). In contrast to strong electrostatic and hydrogen bonding inner forces, the interactions between the chords in the crystal are governed exclusively by weak van der Waals forces. This can be seen from the shortest interatomic distances between the neighboring chords, which are 2.82 Å for H···H and 4.055(8) Å for C···C contacts. These distances significantly exceed the sums of van der Waals radii [13] of 2.4 and 3.4 Å, respectively. A two-fold crystal axis of symmetry passes through the center of the chord.

Summarizing the results it is clear that the structural units in **Rim HCl** crystals show strong interatomic interactions along the crystallographic *c* axis and weak interactions in the two other crystallographic directions. In other words, the atomic arrangement, that is the crystal structure, suggests anisotropy of the physical properties in the solid.

The dimensions of the **Rim HCl** crystals, measured with the help of a light microscope (Fig. 2), gave high values for the aspect ratio in the range of 35 – 40. Indexing the crystal faces with XRD demonstrated that the shape of the **Rim HCl** crystals can be well defined by a simple geometric form of a parallelepiped with lateral faces having Miller indices (1 1 0) and (1 $\bar{1}$ 0), the top face being (0 0 1) as shown in Fig. 5. It should be emphasized that the maximal dimension of the needle-like crystals coincides with the direction of the unit cell *c* axis.

Results from PXRD confirmed the XRD determination of the crystal faces (1 1 0) and (1 $\bar{1}$ 0), which are equivalent because the structure factors $F(hk0)$ and $F(h\bar{k}0)$ are equal for the space group $P4_2bc$. The theoretical diffraction pattern (A), simulated [14] from atomic coordinates in the unit cell, the experimental (B) powder diffraction pattern and the experimental PXRD pattern (C) from a single crystal face (1 1 0) of **Rim HCl** are presented in Fig. 6. One can see that the experimental peaks from the single crystal (1 1 0) face correspond well to equivalent peaks (1 1 0), (2 2 0), (3 3 0), (4 4 0) and (5 5 0) in the experimental and simulated powder patterns. Fig. 6 also assures that the raw material does not contain another polymorph [15] of **Rim HCl** after recrystallization from dimethylsulfoxide at 50 °C, and the single crystals contain the same polymorphic form as in the commercially offered powder.

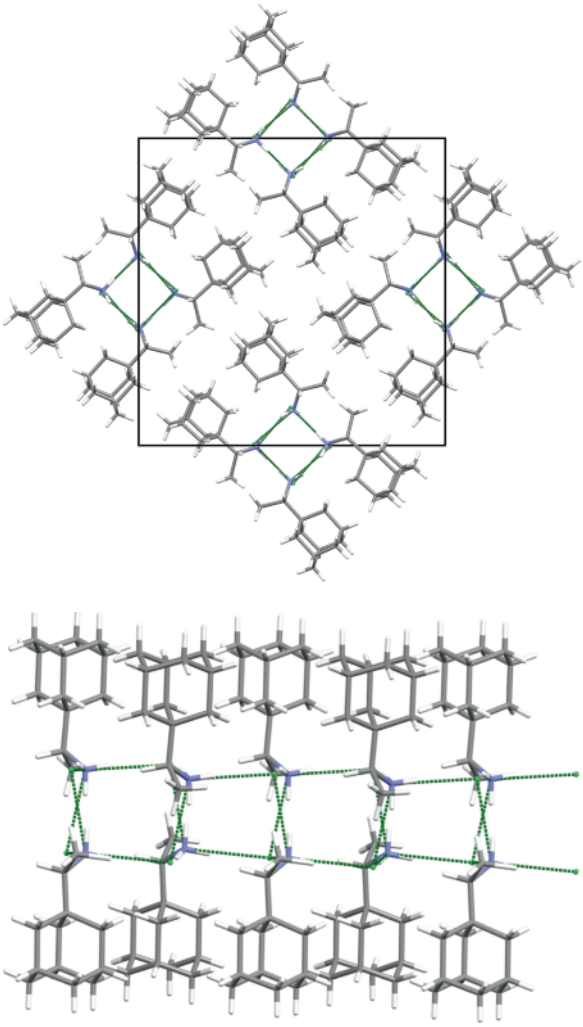

Fig. 4 (color online). (a) Projection of the structure viewed down the *c* axis. (b) Projection of the structure along $(a+b)$ vector.

It is known that the habit of a crystal is determined by the various growth rates of the different faces of the crystal under different internal and external conditions. Internal conditions that affect the habit of a crystal include factors such as impurity content and liq-

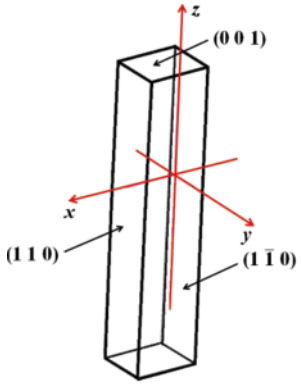

Fig. 5. Results of XRD indexing of the crystal faces.

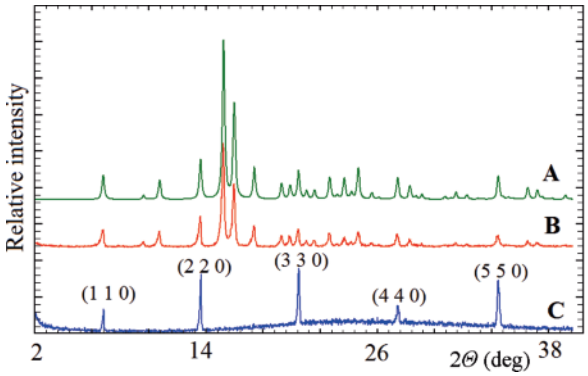

Fig. 6. PXRD patterns calculated from single-crystal data (**A**), experimental of the raw material (**B**) and experimental from a single crystal face (1 1 0) (**C**).

uid occlusions, while external factors include temperature and solution flow around a crystal [7]. Leaving aside crystallization conditions which we did not study in this work, we explain the crystal habit from data on the atomic level. As it was already mentioned, the knowledge of crystal structure and indices of crystal faces provides information on functional chemical groups that are exposed on the surface of the crystal faces. In the **Rim HCl** structure the surface of the fastest growing face (0 0 1) contains positively charged NH_3^+ groups able to adopt new Cl^- anions and rimantadinium cations from the solution. On the contrary, the surfaces of faces (1 1 0) and (1 $\bar{1}$ 0) contain aliphatic adamantane fragments exhibiting weak interatomic interactions. Since the energy of the electrostatic and hydrogen bonding interactions considerably exceeds the energy of the van der Waals interactions it is natural that crystals of **Rim HCl** grow faster in the *c* axis direction, resulting in the needle-like habit. In the same way anisotropy in interatomic interactions explains the reduction of long-range order in the crystal structure and of the X-ray crystallinity under the application of low temperatures.

Conclusion

The crystal structure of the antiviral drug rimantadine hydrochloride was studied for the first time by single-crystal X-ray structure analysis. This crystalline solid presents an interesting example of structure-physical properties relationship. We have attempted to use the knowledge of the crystal structure and the indices of the crystal faces of the antiviral drug **Rim HCl** to explain the high aspect ratio of its crystals and some mechanical and thermal properties. The structural units in **Rim HCl** crystals have strong interatomic interactions along the crystallographic *c* axis and weak interactions in the other two directions. The direction of the crystallographic *c* axis coincides with the maximum dimension of the needle-like crystals. This atomic arrangement explains the anisotropy of the physical properties of the solid and the observations made upon slicing and cleavage of the crystals: the cut edges of the crystals were stratified, and cracking of the crystals resulted in their bursting into smaller needles with a similar aspect ratio. The crystal structure explains also the low X-ray diffraction quality and an increase of the mosaicity upon application of low temperatures.

Experimental Section

Rimantadine hydrochloride was donated by JSC Grindeks. Dimethylsulfoxide was purchased from Rigas Kimija Ltd. Both, **Rim HCl** and dimethylsulfoxide were used without further purification. **Rim HCl** (30 mg, 0.14 mmol) was dissolved in 1 mL dimethylsulfoxide. Slow evaporation of the solvent at 50 °C gave crystals suitable for single-crystal X-ray diffraction analysis. Experimental and refinement details of the X-ray diffraction study are summarized in Table 2.

X-Ray structure determination

It should be noted that the main problem with the **Rim HCl** crystal structure solution was the determination of the

correct space group due to high mosaicity. First we solved the structure in the orthorhombic space group $Pc2a$, with two molecules in the asymmetric unit and $a = 18.2180(12)$, $b = 7.4930(6)$, $c = 18.1980(16)$ Å, $V = 2484.2(3)$ Å^3, $M = 215.76$, $D_x = 1.15$ g cm^{-3}, $Z = 4$, $Z' = 2$, $F(000) = 944$. However, the refinement gave high R factors ($R1 = 0.0969$ [$I > 2\ \sigma(I)$]). A considerable number of crystals of **Rim HCl** were examined for their X-ray diffraction quality. The best one was tetragonal, space group $P4_2bc$, with the unit cell parameters $a = 18.3774(8)$, $c = 7.5049(2)$ Å, $Z = 8$, $V = 2534.6(2)$ Å^3.

Diffraction intensities were measured at room temperature, because it was discovered that low temperatures damage the quality of the crystals.

H atoms bound to C atoms were positioned geometrically, with C–H = 0.96 – 0.98 Å, and refined as riding, with $U_{iso}(H) = 1.2$ or 1.5 $U_{eq}(C)$. One of the H atoms bound to the N atom was included in a position identified from difference Fourier maps and was then refined as riding, with $U_{iso}(H) = 1.2\ U_{eq}(N)$. The other two H atoms were refined with the N–H distance restrained to 0.87 Å and with $U_{iso}(H) = 1.2\ U_{eq}(N)$.

The reflection intensities were measured on a Bruker Nonius KappaCCD diffractometer with graphite-monochromatized MoK_α radiation ($\lambda = 0.71073$ Å). The data collection was performed using the KappaCCD Server Software [16], the cell refinement was done with SCALEPACK [17], and the data were reduced by DENZO and SCALEPACK [17]. The structure was solved by Direct Methods using SIR2004 [18] and refined anisotropically on F^2 values using SHELXL-97 [19 – 21].

The crystals were indexed using the program COLLECT [16]. Crystal face indices were assigned relative to the $P4_2bc$ cell setting with the aid of a video capture utility within the program COLLECT [16]. Miller indices of well-defined faces were deduced by inspection of the crystal viewed along specific real and reciprocal space vectors.

Table 2. Crystal structure and refinement data for **Rim HCl**.

Empirical formula	$C_{12}H_{22}N^+\ Cl^-$
M_r	215.76
Crystal size, mm^3	$0.42 \times 0.10 \times 0.10$
Crystal system	tetragonal
Space group	$P4_2bc$
a, Å	18.3774(8)
c, Å	7.5049(2)
V, Å^3	2534.6(2)
Z	8
$D_{calcd.}$, g cm^{-3}	1.13
μ(MoK_α), cm^{-1}	2.7
$F(000)$, e	944
hkl range	$-27 \le h \le 27$, $-18 \le k \le 18$, $-8 \le l \le 11$
$((\sin\theta)/\lambda)_{max}$, Å^{-1}	0.7456
Refl. measured/unique/R_{int}	7534/4057/0.130
Param. refined	138
$R(F)$ / $wR(F^2)$ (all refl.)	0.060/0.165
x(Flack)	0.26(12)
GoF (F^2)	0.92
$\Delta\rho_{fin}$ (max/min), e Å^{-3}	0.16/−0.14

CCDC 971974 contains the supplementary crystallographic data for this paper. These data can be obtained free of charge from The Cambridge Crystallographic Data Centre *via* www.ccdc.cam.ac.uk/data_request/cif.

Powder X-ray diffraction

Powder X-ray data were obtained on Rigaku ULTIMA IV powder diffractometer (CuK_α $\lambda = 1.5418$ Å, 40 kV, 40 mA) using the parallel beam method. Data were collected at 291 K with 0.02° steps and a scan speed of 0.1° per min.

Acknowledgement

This work was supported by the European Regional Development Fund (no. 2DP/2.1.1.1.0/10/APIA/VIAA/066).

[1] L. Simeonova, G. Gegova, A. S. Galabov, *Antivir. Res.* **2012**, *95*, 172 – 182.
[2] S. Bantia, D. Kellogg, C. D. Parker, Y. S. Babu, *Antivir. Res.* **2010**, *88*, 276 – 280.
[3] T. Horimoto, Y. Kawaoka, *Nat. Rev. Microbiol.* **2005**, *3*, 591 – 600.
[4] A. Borsos, B. G. Lakatos, *Chem. Eng. Res. Des.* **2014**, *92*, 1133 – 1141.
[5] Y. Bao, J. Zhang, Q. Yin, J. Wang, *J. Cryst. Growth* **2006**, *289*, 317 – 323.
[6] B. Biscans, *Powder Technol.* **2004**, *143 – 144*, 264 – 272.
[7] D. B. Patience, J. B. Rawlings, *AIChE J.* **2001**, *47*, 2125 – 2130.
[8] W. Kaminsky, *J. Appl. Crystallogr.* **2007**, *40*, 382 – 385.
[9] A. J. Hlinak, K. Kuriyan, K. R. Moriss, G. V. Reklaitis, P. K. Basu, *J. Pharm. Innov.* **2006**, *1*, 12 – 17.
[10] C. C. Aubrey-Medendorp, S. Parkin, T. Li, *J. Pharm. Sci.* **2008**, *97*, 1361 – 1367.
[11] C. K. Johnson, M. N. Burnett, ORTEP-III (version 1.0.2), Rep. ORNL-6895, Oak Ridge National Laboratory, Oak Ridge, TN (USA) **1996**. Windows version: L. J. Farrugia, University of Glasgow, Glasgow, Scot-

land (UK) **1999**. See also: L. J. Farrugia, *J. Appl. Crystallogr.* **1997**, *30*, 565.
[12] F. H. Allen, O. Kennard, D. G. Watson, L. Brammer, A. G. Orpen, R. Taylor, *J. Chem. Soc., Perkin Trans. 2* **1987**, S1–S19.
[13] S. S. Batsanov, *Inorg. Mater.* **2001**, *37*, 1031 – 1046.
[14] C. F. Macrae, I. J. Bruno, J. A. Chisholm, P. R. Edgington, P. McCabe, E. Pidcock, L. Rodriguez-Monge, R. Taylor, J. van de Streek, P. A. Wood, *J. Appl. Crystallogr.* **2008**, *41*, 466 – 470.
[15] J. van de Streek, S. Motherwell, *Acta Crystallogr.* **2005**, *B61*, 504 – 510.
[16] KappaCCD Server Software. Nonius BV, Delft (The Netherlands) **1997**.
[17] Z. Otwinowski, W. Minorin *Methods in Enzymology*, Vol. 276, *Macromolecular Crystallography*, Part A (Eds.: C. W. Carter, Jr., R. M. Sweet), Academic Press, New York, **1997**, pp. 307 – 326.
[18] M. C. Burla, R. Caliandro, M. Camalli, B. Carrozzini, G. L. Cascarano, L. De Caro, C. Giacovazzo, G. Polidori, R. Spagna, *J. Appl. Crystallogr.* **2004**, *38*, 381 – 388.
[19] G. M. Sheldrick, SHELXS/L-97, Programs for Crystal Structure Determination, University of Göttingen, Göttingen (Germany) **1997**.
[20] G. M. Sheldrick, *Acta Crystallogr.* **1990**, *A46*, 467 – 473.
[21] G. M. Sheldrick, *Acta Crystallogr.* **2008**, *A64*, 112 – 122.